ACS OMEGA

Open Access

http://pubs.acs.org/journal/acsodf

Article

Excitation Wavelength Optimization of Europium-Doped Carbon Dots (Eu-CDs) for Highly Sensitive Detection of Tetracyclines in Water

Aigerim Babenova,[⊥] Kamila Zhumanova,[⊥] Ainur Zhussupbekova, Kuanysh Zhussupbekov, Daniele Tosi, and Timur Sh. Atabaev*

Cite This: *ACS Omega* 2025, 10, 619−626

Read Online

ACCESS | Metrics & More | Article Recommendations | Supporting Information

ABSTRACT: Antibiotic contamination of water bodies has become a serious problem, which leads to aquatic life pollution and the development of antibiotic resistance. Hence, development of highly sensitive and selective optical sensors for antibiotic detection is at the forefront of scientific research. In this study, we present the synthesis of europium-doped carbon dots (Eu-CDs) and excitation wavelength optimization for the highly sensitive detection of tetracycline (TC) and TC-family antibiotics in water. An extensive physicochemical analysis and excitation wavelength optimization reveal that Eu-CDs can yield an exceptionally high limit of detection of TC at ∼5.8 nM over a linear range of 0.01−3 μM. Selectivity analysis with other common antibiotics revealed that the produced Eu-CDs are highly sensitive to TC and TC-group antibiotics only. A plausible mechanism for excitation-dependent TC detection by Eu-CDs is proposed. We firmly believe that the prepared Eu-CDs can be potentially employed for quick and sensitive monitoring of TC-family antibiotics in water samples.

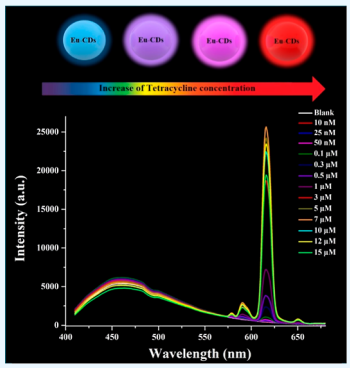

1. INTRODUCTION

Tetracycline (TC) is a frequently employed antibiotic thanks to its broad spectrum of activity against Gram-positive/Gram-negative bacteria and a number of other pathogens in veterinary medicine.[1] Furthermore, TC is extensively employed as a growth promoter for swine, poultry, and aquaculture.[2,3] On the other hand, TC is not completely digested by living beings; therefore, around 69−86% of TC is excreted through urine and feces.[4] Following that, TC goes to soil and eventually contaminates the neighboring water reservoirs.[4−6] According to toxicological studies, the presence of TC and its derivatives in water bodies has several adverse effects, such as inhibiting root formation and plant growth, suppressing the chloroplast system and the plasmolysis function of green algae, promoting oxidative stress in cyanobacteria, development of anomalies in aquatic life creatures, and generating antibiotic-resistant bacteria.[1,3]

The conventional method of TC detection involves high-performance liquid chromatography coupled with mass spectrometry.[7,8] However, this method of detection is associated with substantial operational expenses, such as high electrical energy consumption, operator training, special sample preparation, and impracticality for on-site use. In this regard, fluorescence-based detection techniques can be considered as a possible solution to the issues associated with HPLC-TC usage. For example, a portable spectrophotometer with an autonomous power supply may analyze water on-site in a matter of minutes. Moreover, no special operator training or substantial sample preparation is usually necessary.

Various optical agents based on carbon quantum dots (CDs) for quantitative determination of TC in aqueous solutions have been proposed recently. For example, Table S1 (Supporting Information) lists the detection range and limit of detection (LOD) for several unmodified CDs published recently. Despite their low cost, some of these produced CDs were not tested against other possible interference molecules/ions in water and yielded high LOD values in most of the cases. On the other hand, some CDs contain europium (Eu) element, which can specifically be linked to TC with the formation of an organometallic chelate.[9,10] Upon light stimulation, energy transfer between the TC ligand and the Eu atom causes changes in the emission pattern, which can be detected and quantified as a function of TC concentration. To date, Eu-doped metal−organic frameworks and Eu-doped CDs are gaining popularity for TC detection owing to their simplicity of production, strong optical signals, and excellent stability.[11−16] Among these two forms of optical agents, Eu-doped carbon dots can be made using "green" chemistry concepts that do not

Received: August 12, 2024
Revised: December 5, 2024
Accepted: December 6, 2024
Published: December 22, 2024

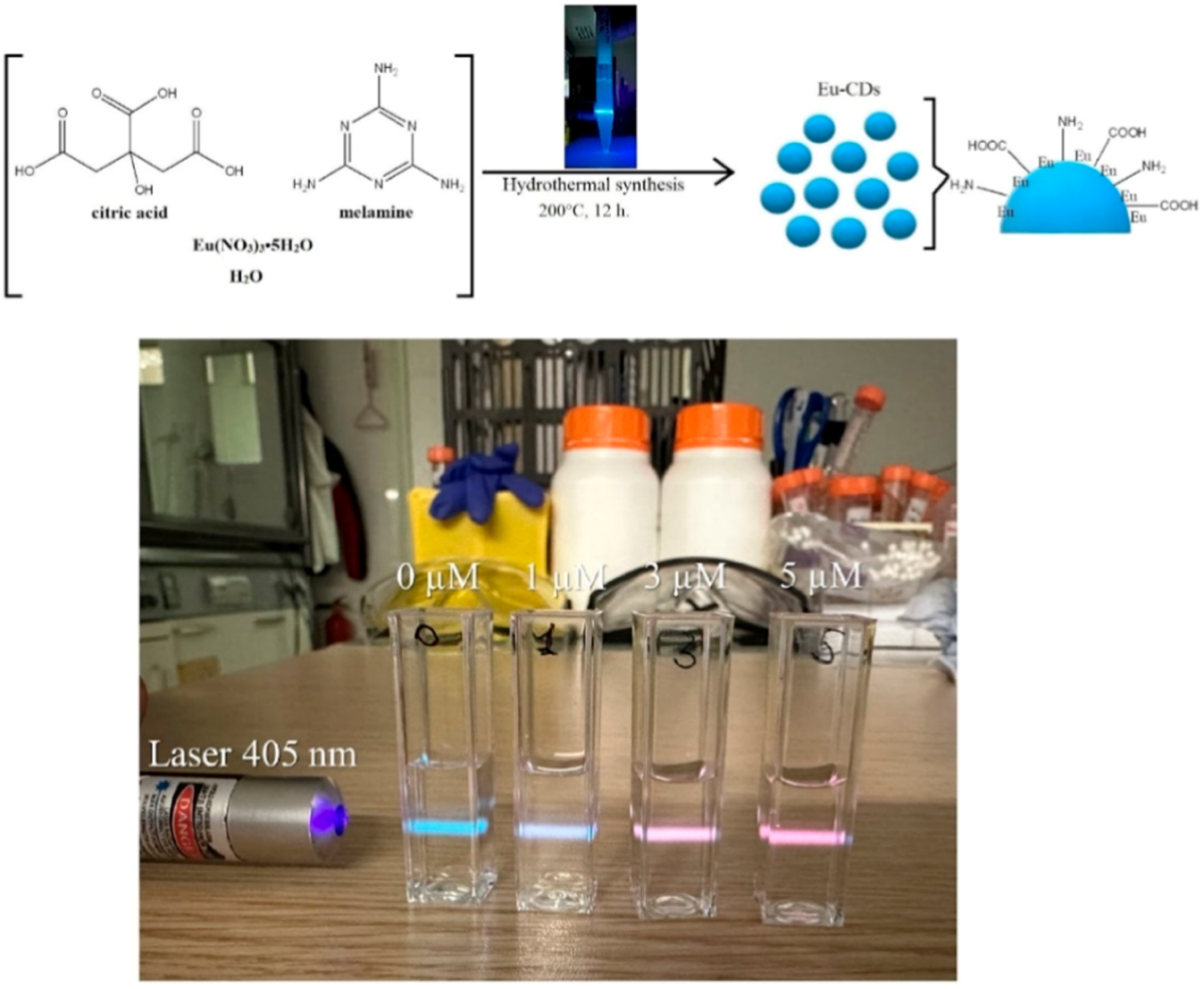

Figure 1. General scheme showing the synthesis of Eu-CD synthesis and colorimetric detection of TC in water.

require the use of large amounts of chemicals or toxic solvents. Consequently, Eu-doped carbon dots generated from various carbon-rich precursors frequently appear in the scientific literature. However, the authors of these studies often use the excitation wavelengths in the region of ∼350−370 nm that are considered to be optimal for achieving strong emission signals from CDs. However, the europium ions are typically activated in the range of 390−400 nm, which is associated with direct $^7F_0 \rightarrow {}^5L_6$ transitions in surface-located Eu^{3+} ions.[17,18] It is reasonable to assume that the sensing potential of various Eu-doped CDs has not been fully utilized and should be explored further. Hence, the main aim of this study is to prepare Eu-doped CDs and optimize the excitation wavelength for the highly sensitive detection of TC-based antibiotics in water. As a result of excitation wavelength adjustment, we achieved LOD of ∼5.8 nM for TC, which is likely one of the lowest among Eu-doped CDs and other optical sensors for TC detection reported to date.

2. MATERIALS AND METHODS

2.1. Synthesis of the Eu-CDs. High-purity reagents were purchased from Merck and used without any purification. The synthesis of Eu-doped CDs was carried out using a hydrothermal method. In brief, citric acid (0.2 g), melamine (0.1 g), and $Eu(NO_3)_3 \times 5H_2O$ (21.4 mg) were dissolved in 10 mL of deionized (DI) water. The prepared solution was then placed in a stainless steel autoclave with a Teflon liner (capacity of 25 mL) and heated in a muffle oven at 200 °C for 12 h. After cooling to ambient temperature, the produced solution was filtered using a 0.22 μm syringe filter and dialyzed for 24 h using a 1 kDa dialysis membrane to eliminate any unreacted reagents. The Eu-CD solution was freeze-dried and collected as a powder for further examination.

2.2. Characterization of the Eu-CDs. The morphology and size distribution of Eu-CDs were analyzed using JEM 1400 Plus transmission electron microscopy (TEM, JEOL Ltd.). The Fourier transform infrared (FTIR) analysis of Eu-CDs was performed by using the Nicolet iS10 spectrometer (Thermo Fisher Scientific Inc.). The optical properties of Eu-CDs were tested using an RF-6000 spectrophotometer (Shimadzu Corporation) and a Quantaurus absolute quantum yield spectrometer (Hamamatsu Photonics K·K.). The surface analysis of Eu-CDs was performed using an Omicron MultiProbeX-ray photoelectron spectrometer (XPS, Scienta Omicron). The concentration of europium dopant and

https://doi.org/10.1021/acsomega.4c07414
ACS Omega 2025, 10, 619−626

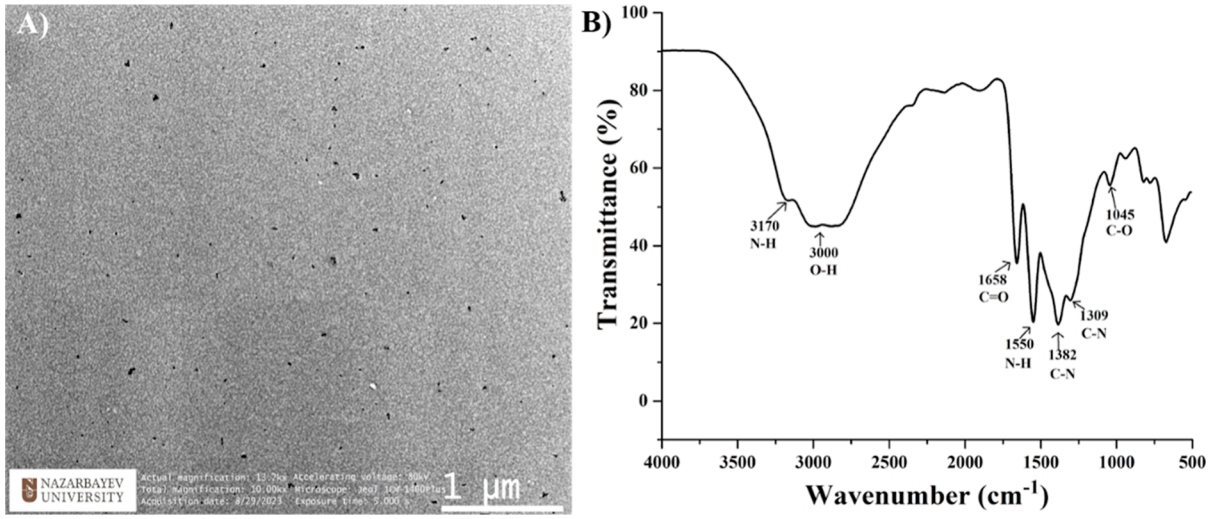

Figure 2. TEM micrograph (A) and FTIR survey (B) of Eu-CDs.

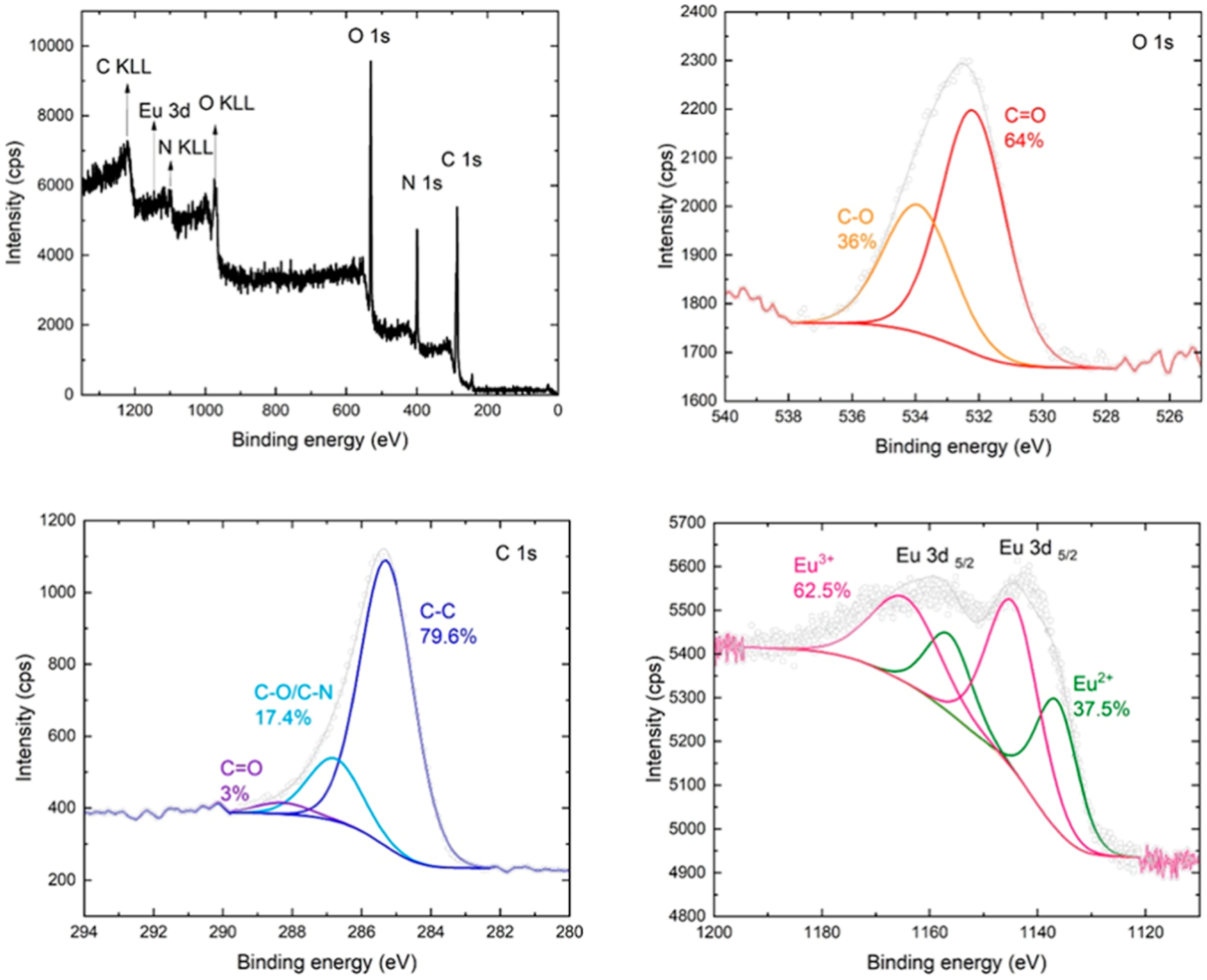

Figure 3. Full XPS survey and high-resolution XPS survey of O 1s, C 1s, and Eu 3d regions.

determination of elements in tap water have been performed using an iCAP 6300 Duo inductively coupled plasma optical emission spectroscopy (ICP-OES, Thermo Fisher Scientific Inc.).

2.3. TC Detection with the Eu-CDs. For TC detection, a stock solution of TC (1 mM) was prepared first. Subsequently, the stock solution was diluted to concentrations ranging from 10 nM to 15 μM. For TC detection, 2 mL of each TC concentration solution was added to the cuvette containing 100 μL of Eu-CD solution with a concentration of 20 μg/mL. The TC concentration was determined by using the red peak fluorescence at 615 nm. LOD was calculated using the standard method, i.e., LOD = $3\sigma/S$, where σ is the standard deviation of the measurements and S is the slope of the

https://doi.org/10.1021/acsomega.4c07414
ACS Omega 2025, 10, 619−626

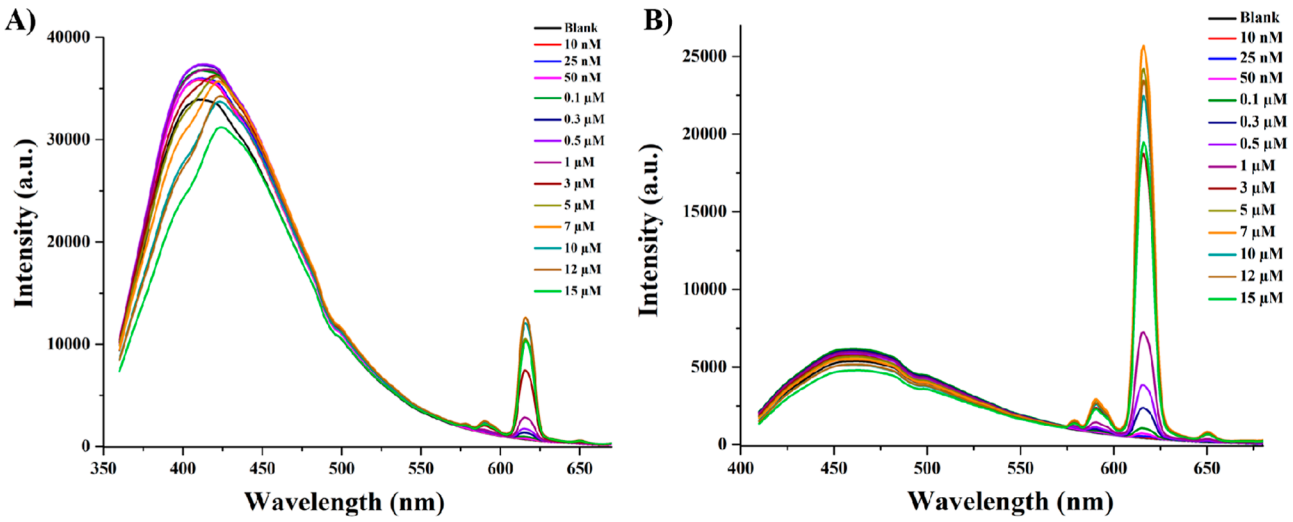

Figure 4. PL emission of Eu-CDs at different TC concentrations at λ_{exc} = 341 nm (A) and λ_{exc} = 390 nm (B).

calibration curve. All experiments were repeated three times at room temperature to ensure reproducibility of the results.

2.4. Selectivity and Stability Analysis. Various antibiotics, including ciprofloxacin (CIP), ampicillin (AMP), streptomycin sulfate (STM), erythromycin (ERY), doxycycline monohydrate (DOX), chlortetracycline hydrochloride (CTC), amoxicillin trihydrate (AX), chloramphenicol (CHL), oxytetracycline (OTC), kanamycin (KAN), and lincomycin (LIN), were tested for selectivity analysis. The concentration of each antibiotic was fixed at 3 μM (the upper limit of the linear TC detection range). The pH stability of Eu-CDs was tested in the range of 5−9 by adjusting the pH of the TC solution. Salinity tolerance was tested through the addition of an aqueous solution of NaCl with a concentration of 100 ppm.

3. RESULTS AND DISCUSSION

Figure 1 shows the general hydrothermal synthesis of Eu-CDs and their further application for TC detection. During the carbonization process, Eu (III) ions were trapped in the core and surface of CDs. The presence of TC in water activates the surface-located Eu (III) ions, resulting in a gradual color-tuning of emission. The red peak intensity associated with transitions within the Eu (III) is well correlated with TC concentration in water, making Eu-CDs suitable for colorimetric TC detection. Figure 2A depicts a TEM micrograph of the as-prepared Eu-CDs. One can observe that Eu-CDs are quasi-spherical black dots with diameters ∼10 ± 3 nm according to the size analysis by ImageJ software (Figure S1 and Supporting Information). ICP-OES analysis of the as-prepared Eu-CDs confirmed the presence of Eu element at a concentration of ∼1.73 wt %.

Figure 2B shows the FTIR spectra of Eu-CDs revealing a stretching and bending vibration of N−H at 3170 and 1550 cm^{-1}, respectively.[19−22] The broad and intense absorption band at 3000 cm^{-1} suggests the presence of the stretching vibration of the O−H bond.[19−22] The characteristic bands at 1658 and 1045 cm^{-1} confirmed the existence of C═O and C−O vibrations,[19−22] whereas intensive bands at 1382 and 1309 cm^{-1} can be assigned to aromatic tertiary amine and aromatic secondary amine C−N stretching vibrations.[23] Thus, FTIR analysis confirmed that the produced Eu-CDs consisted of a carbon backbone with different functional groups on the surface.

XPS analysis was further employed to characterize the Eu-CDs. The full XPS survey revealed core-level peaks corresponding to C 1s, N 1s, O 1s, and Eu 3d as it is shown in Figure 3.[19−22] Core-level regions were analyzed by using CasaXPS software. The high-resolution C 1s spectrum indicates three distinct components: C−C/C═C bonds at 285.2 eV (79.6%), C−O/C−N at 286.7 eV (17.4%), and C═O/C═N at 288.3 eV (3%).[19−22] The narrow O 1s spectrum displays two peaks at 532.1 eV (64%) and 533.3 eV (36%), corresponding to C−O and C═O bonds, respectively.[19−22] The high-resolution Eu 3d spectra show two doublet peaks (Eu 3d5/2 and Eu 3d3/2), which can be deconvoluted into Eu^{2+} (∼37.5%) at 1136.4 and 1156.4 eV and Eu^{3+} (62.5%) at 1144.5 and 1164.5 eV.[24,25] The Eu 3d deconvoluted by applying a spin−orbit splitting of approximately 20 eV between the 3d5/2 and 3d3/2 components, with an area ratio of 3:2 for the 3d3/2 and 3d5/2. A Shirley background correction was employed during the fitting process to ensure accurate peak deconvolution.

The optical properties of Eu-CDs were further assessed by PL spectroscopy. Figure S2 (Supporting Information) confirms the excitation-dependent behavior of Eu-CDs, i.e., demonstrating the red-shifting of emission spectra as the excitation wavelength is gradually increased from 320 to 380 nm. In general, excitation-dependent properties of CDs are often described with size variation and presence of various functional groups of the CD surface. This is consistent with the provided data, i.e., prepared Eu-CDs vary in size and have numerous surface functional groups, as confirmed by size, FTIR, and XPS measurements. One can clearly notice that Eu-CDs emit only in the blue-green region as shown by the emission spectra measured in the range of 380−700 nm. The as-prepared Eu-CDs exhibited the highest emission peak at 422 nm (λ_{exc} = 341 nm), with an absolute quantum yield of ∼14.4%. When TC is added to the solution, TC coordinates to surface-located Eu^{3+} ions with the formation of a stable TC−Eu^{3+} complex and a new peak with a maximum at ∼615 nm appears thanks to $^5D_0 \rightarrow {}^7F_2$ transition of Eu^{3+}. Generally, coordinated TC acts as "antennae" by absorbing light energy and transferring it to Eu^{3+} ions which in turn facilitate the red emission to occur.[25,26] As a proof of concept, emission of Eu-CDs in bare DI water and DI

https://doi.org/10.1021/acsomega.4c07414
ACS Omega 2025, 10, 619−626

water containing 1 μM TC is depicted in Figure S3A (Supporting Information). The red signal appears solely in the presence of TC, indicating the formation of the TC−Eu^{3+} complex and the energy transfer from TC to Eu^{3+}. On the other hand, pure CDs are not showing a red signal in water with/without TC (Figure S3B, Supporting Information), confirming the beneficial role of Eu^{3+} dopant for colorimetric TC detection. Figure S4 (Supporting Information) shows the intensity variation of $^5D_0 \rightarrow {}^7F_2$ transition upon excitation with various wavelengths in a solution with a fixed concentration of TC. The excitation range was selected from 370 to 410 nm which is close to the $^7F_0 \rightarrow {}^5L_6$ transition in Eu^{3+}. Moreover, λ_{exc} = 341 nm was also tested as the optimal excitation wavelength for Eu-CDs in the absence of TC in solution. The intensity of the $^5D_0 \rightarrow {}^7F_2$ transition increases with increasing excitation wavelength, reaching a maximum at λ_{exc} = 390 nm and then progressively decreasing. The intensity of the $^5D_0 \rightarrow {}^7F_2$ transition at λ_{exc} = 341 nm was substantially lower as compared to λ_{exc} = 390 nm, which was selected further as the optimal excitation wavelength for TC detection.

Figure 4A,B shows the PL emission of Eu-CDs as a function of the TC concentration in solution excited at λ_{exc} = 341 nm and λ_{exc} = 390 nm, respectively. In both cases, the emission bands in the red region are associated with $^5D_0 \rightarrow {}^7F_j$ (with j = 0, 1, 2, and 3) transitions in Eu^{3+}.[27,28] Examining the intensity of the most prominent $^5D_0 \rightarrow {}^7F_2$ transition at ∼615 nm reveals a significant difference between the two excitation wavelengths. In particular, all bands associated with Eu^{3+} transitions become more intense and apparent at λ_{exc} = 390 nm. This observation also applies to very small TC concentrations, ranging from 10 to 100 nM (Figure S5 and Supporting Information), making them easier to resolve and quantify. Figure 5 compares the intensity of the $^5D_0 \rightarrow {}^7F_2$

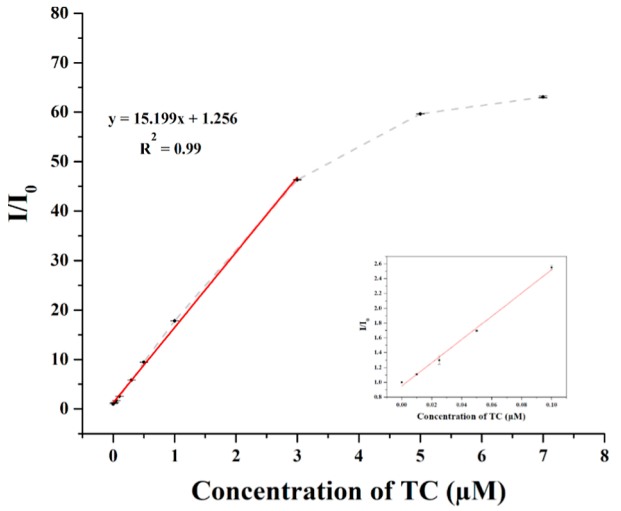

Figure 5. I/I_0 plot of Eu-CDs monitored at 615 nm with various TC concentrations.

transition in Eu-CDs (I, at 615 nm) to the intensity of the blank solution (I_0, without TC) at different TC concentrations (0−7 μM). One can notice that the linear detection of TC under λ_{exc} = 390 nm is maintained in the range of 0.01−3 μM (R^2 = 0.99). The LOD was determined to be ∼5.8 nM. One can also observe that the fluorescence signal at 615 nm decreases at high TC concentrations (≥10 μM). We can speculate that the quenching mechanism is highly likely to be static due to the formation of a stable Eu−TC complex and gradual saturation of the red signal at high TC concentrations. On the other hand, the exact quenching mechanism should be evaluated using time-resolved PL spectroscopy which can be addressed in future studies. Table 1 compares the composition,

Table 1. Composition, Detection Range, and LOD of Some Eu-Based Structures for TC Detection

composition (method)	detection range	LOD	reference
Eu-MOF (fluorescence intensity)	2.5−12.50 μM	225 nM	12
Eu-CQDs (fluorescence intensity)	0.5−200 μM	300 nM	13
CDs-Eu (ratiometric fluorescence)	0−3.5 μM	11.7 nM	14
Eu-CDs (ratiometric fluorescence)	0−100 μM	6.90 nM	15
Eu-CDs (ratiometric fluorescence)	0−624 μM	15.8 nM	16
CDs from carp roe (fluorescence intensity)	0.1−50 μM	40.0 nM	19
Cu-CDs−COOH−Eu (fluorescence intensity)	0.4−60 μM	36.1 nM	25
Eu/CPDs (fluorescence intensity)	0.05−56 μM	16.4 nM	26
GQDs-Eu (ratiometric fluorescence)	0−20 μM	8.20 nM	31
C-g-C_3N_4−Eu (ratiometric fluorescence)	0.01−40 μM	7.70 nM	32
Eu-CDs (fluorescence intensity)	0.01−3 μM	5.80 nM	this study

linear range, and LOD of various Eu-CDs and Eu-based structures for TC detection reported to date. Despite the smaller detection range, it is clear that the LOD of Eu-CDs reported in this work is better than that of other structures reported so far. On the other hand, the real TC concentrations in wastewater effluents across the Europe typically vary from 1.24 to 12.34 μg L^{-1} (∼2.8−27.8 nM).[29] In addition, Pena and coauthors found that TC concentrations in hospital effluents ranged from ∼6 to 531.7 μg L^{-1} (∼13.51 nM−1.2 μM), while TC concentrations in municipal wastewater treatment plants were in the range of 95.8−915.3 μg L^{-1} (∼0.22−2.06 μM).[30] Hence, the detection range of ∼0.01−3 μM is sufficient for TC detection in real water samples, while reliable TC detection at lower concentrations requires a lower LOD that can be achieved by excitation wavelength optimization.

The next step consisted of assessing the selectivity of Eu-CDs with different antibiotics (λ_{exc} = 390 nm and λ_{em} = 615 nm). Figure S6 (Supporting Information) reveals that, under the same conditions, Eu-CDs are selective for TC-family antibiotics only (TC, OTC, DOX, and CTC) and less susceptible to other antibiotics. A similar feature was also observed in other reports;[14,16] hence, prepared Eu-CDs can be considered selective to TC-family compounds only. Figure S7 (Supporting Information) shows the corresponding detection ranges and slightly higher LOD for the OTC, DOX, and CTC antibiotics. It was found that OTC, DOX, and CTC can also be detected in the range of 0.01−3 μM, which is typically enough for detection in hospital effluents and municipal wastewater. Figure S8 (Supporting Information) shows that the optimal pH for TC sensing purposes is 7. At lower pH, excited electrons can be transferred to H^+ in solution, causing the fluorescence emission to decrease. Excessive OH^- groups at higher pH can also cause fluorescence quenching because

https://doi.org/10.1021/acsomega.4c07414
ACS Omega 2025, 10, 619−626

the OH^- group is known as the luminescence quencher for numerous optical structures.[33] It has also been found that TC detection is unaffected by water salinity (NaCl, 100 ppm), and TC detection can be realized, similar to that at pH = 7. Hence, the proposed Eu-CDs can be reliably employed for sensitive monitoring of TC-family antibiotics in drinking water. On the other hand, one can also explore other separation and purification techniques, such as column chromatography, since this step may potentially affect the sensitivity of the Eu-CDs to TC-based antibiotics.[34,35]

To demonstrate the applicability of Eu-CDs for TC detection in real samples, tap water has been collected in Astana city (51.1655° N, 71.4272° E), filtered by a 0.45 μm filter, and analyzed by ICP-OES for elemental concentration (Table S2, Supporting Information). Next, aqueous solutions of TC with certain concentrations have been prepared using this filtered tap water. The pH of the solution has been raised to 10 using diluted NaOH to precipitate some heavy ions that may quench the optical signals of Eu-CDs. Formed precipitates have been removed by centrifugation, and the pH of the supernatant has been adjusted to 7 again using diluted HCl. The analysis of TC in the real sample (Table 2) reveals a good recovery with a relative standard deviation less than 4%. Figure S9 (Supporting Information) shows that no red signal was detected using Eu-CDs in treated TC-free tap water.

Table 2. TC Detection in Real Samples (Tap Water)

added TC (μM)	detected TC (μM)	recovery (%)	RSD (%)
0.5	0.48	96	2.9
1	0.97	97	2.6
2	1.93	96.5	3.1

The excitation-dependent sensing mechanism of Eu-CDs can be explained using the optical level diagram of Eu^{3+}. Figure 6 shows that λ_{exc} = 390 nm directly populates the $^5L_6$ level,

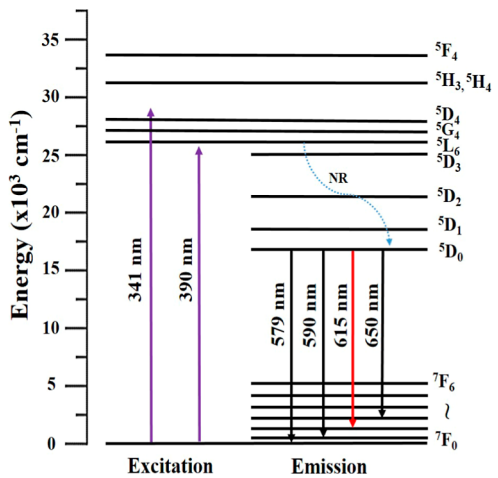

Figure 6. Optical level diagram showing the excitation and emission transitions in Eu^{3+}.

which is nonradiatively relaxed to the $^5D_0$ level and where emission associated with $^5D_0 \rightarrow {}^7F_j$ (with j = 0, 1, 2, and 3) transitions occurs. In contrast, λ_{exc} = 341 nm can populate the $^5D_4$ level, resulting in an additional nonradiative relaxation pathway where some of the electrons can be lost. Furthermore, λ_{exc} = 341 nm is favorable for excitation of some functional groups on the surface of CDs, resulting in the appearance of a broad emission band in the region of ~350−550 nm as shown in Figure 4A. Consequently, the reduced number of $^5D_0 \rightarrow {}^7F_j$ transitions results in a weakened emission, influencing the TC sensing capabilities.

4. CONCLUSIONS

In conclusion, we successfully prepared Eu-CDs for the highly sensitive detection of TC and TC-based antibiotics utilizing a fluorescence approach. The key contribution of this study is the optimization of excitation wavelength, resulting in an LOD of ~5.8 nM, which is likely the highest among published literature to date. According to the selectivity analysis, the Eu-CDs agent was selective only to TC and TC-family antibiotics, such as OTC, doxycycline monohydrate (DOX), and chlortetracycline hydrochloride (CTC). A plausible mechanism for excitation-dependent TC detection was proposed. We strongly believe that the excitation-wavelength optimization methodology described in this work can be useful for design of optical sensors with a broad detection range and high sensitivity toward TC-based antibiotics.

■ ASSOCIATED CONTENT

Supporting Information

The Supporting Information is available free of charge at https://pubs.acs.org/doi/10.1021/acsomega.4c07414.

Additional data for size distribution of Eu-CDs; PL excitation and emission analysis of Eu-CDs; monitoring of 615 nm emission of Eu-CDs at different excitation wavelengths, at different TC concentrations, with different antibiotics, and at different pH and salinity; plots of I/I_0 vs antibiotic concentrations for OTC, DOX, and CTC; tap water analysis by ICP-OES; and PL emission of Eu-CDs in tap water without TC (PDF)

■ AUTHOR INFORMATION

Corresponding Author

Timur Sh. Atabaev − *Department of Chemistry, Nazarbayev University, Astana 010000, Kazakhstan;* orcid.org/0000-0001-7252-4098; Email: timur.atabaev@nu.edu.kz

Authors

Aigerim Babenova − *Department of Chemistry, Nazarbayev University, Astana 010000, Kazakhstan*

Kamila Zhumanova − *Department of Chemistry, Nazarbayev University, Astana 010000, Kazakhstan*

Ainur Zhussupbekova − *School of Physics and School of Chemistry, Trinity College Dublin, Dublin 2, Ireland;* orcid.org/0000-0003-2724-8762

Kuanysh Zhussupbekov − *School of Physics and School of Chemistry, Trinity College Dublin, Dublin 2, Ireland; LASSP, Department of Physics, Cornell University, Ithaca, New York 14850, United States;* orcid.org/0000-0003-1909-3270

Daniele Tosi − *Department of Electrical and Computer Engineering, Nazarbayev University, Astana 010000, Kazakhstan;* orcid.org/0000-0002-6500-4964

Complete contact information is available at: https://pubs.acs.org/10.1021/acsomega.4c07414

Author Contributions

⊥A.B. and K.Z. contributed equally to this work. The manuscript was written through contributions of all authors.

https://doi.org/10.1021/acsomega.4c07414
ACS Omega 2025, 10, 619−626

All authors have given approval to the final version of the manuscript.

Notes

The authors declare no competing financial interest.

■ ACKNOWLEDGMENTS

This research was funded by Nazarbayev University FDCRDG (Grant No. 20122022FD4111). A.Z. and K.Z. would like to acknowledge IRC funding through award numbers GOIPD/2022/443 and GOIPD/2022/774 and Erasmus Plus mobility Grants (No. 2018-1-IE02-KA107-000589 and No. 2022-1-IE02-KA171-HED-000079222).

■ REFERENCES

(1) Chopra, I.; Roberts, M. Tetracycline antibiotics: Mode of action, applications, molecular biology, and epidemiology of bacterial resistance. *Microbiol. Mol. Biol. Rev.* **2001**, *65*, 232−260.

(2) Granados-Chinchilla, F.; Rodríguez, C. Tetracyclines in food and feeding stuffs: From regulation to analytical methods, bacterial resistance, and environmental and health implications. *J. Anal. Methods Chem.* **2017**, *2017*, 1315497.

(3) Scaria, J.; Anupama, K. V.; Nidheesh, P. V. Tetracyclines in the environment: An overview on the occurrence, fate, toxicity, detection, removal methods, and sludge management. *Sci. Total Environ.* **2021**, *771*, 145291.

(4) Dai, Y.; Liu, M.; Li, J.; Yang, S.; Sun, Y.; Sun, Q.; Wang, W.; Lu, L.; Zhang, K.; Xu, J.; Zheng, W.; Hu, Z.; Yang, Y.; Gao, Y.; Liu, Z. A review on pollution situation and treatment methods of tetracycline in groundwater. *Sep. Sci. Technol.* **2020**, *55*, 1005−1021.

(5) Zhang, K.; Ruan, R.; Zhang, Z.; Zhi, S. An exhaustive investigation on antibiotics contamination from livestock farms within sensitive reservoir water area: Spatial density, source apportionment and risk assessment. *Sci. Total Environ.* **2022**, *847*, 157688.

(6) Bai, Y.; Wang, Z.; Lens, P. N. L.; Zhussupbekova, A.; Shvets, I. V.; Huang, Z.; Ma, J.; Wu, G.; Zhan, X. Role of iron (II) sulfide in autotrophic denitrification under tetracycline stress: Substrate and detoxification effect. *Sci. Total Environ.* **2022**, *850*, 158039.

(7) Li, Y.; Liu, B.; Zhang, X.; Wang, J.; Gao, S. The distribution of veterinary antibiotics in the river system in a livestock-producing region and interactions between different phases. *Environ. Sci. Pollut. Res.* **2016**, *23*, 16542−16551.

(8) Wang, Z.; Chen, Q.; Zhang, J.; Dong, J.; Yan, H.; Chen, C.; Feng, R. Characterization and source identification of tetracycline antibiotics in the drinking water sources of the lower Yangtze River. *J. Environ. Manage.* **2019**, *244*, 13−22.

(9) Hirsch, L. M.; Van Geel, T. F.; Winefordner, J. D.; Kelly, R. N.; Schulman, S. G. Characteristics of the binding of europium (III) to tetracycline. *Anal. Chim. Acta* **1985**, *166*, 207−219.

(10) Courrol, L. C.; De Oliveira Silva, F. R.; Gomes, L.; Vieira Júnior, N. D. Energy transfer study of europium−tetracycline complexes. *J. Lumin.* **2007**, *122*−*123*, 288−290.

(11) Li, Y.; Wang, J.; Huang, Z.; Qian, C.; Tian, Y.; Duan, Y. An Eu-doped Zr-metal-organic framework for simultaneous detection and removal of antibiotic tetracycline. *J. Environ. Chem. Eng.* **2021**, *9*, 106012.

(12) Wiwasuku, T.; Chuaephon, A.; Puangmali, T.; Boonmak, J.; Ittisanronnachai, S.; Promarak, V.; Youngme, S. Multifunctional fluorescent Eu-MOF probe for tetracycline antibiotics and dihydrogen phosphate sensing and visualizing latent fingerprints. *RSC Adv.* **2023**, *13*, 10384−10396.

(13) Li Liu, M.; Chen, B. B.; Yang, T.; Wang, J.; Dong Liu, X.; Zhi Huang, C. One-pot carbonization synthesis of europium-doped carbon quantum dots for highly selective detection of tetracycline. *Methods Appl. Fluoresc.* **2017**, *5*, 015003.

(14) Shen, Z.; Zhang, C.; Yu, X.; Li, J.; Wang, Z.; Zhang, Z.; Liu, B. Microwave-assisted synthesis of cyclen functional carbon dots to construct a ratiometric fluorescent probe for tetracycline detection. *J. Mater. Chem. C* **2018**, *6*, 9636−9641.

(15) Sang, Y.; Wang, K.; Kong, X.; Cheng, F.; Zhou, C.; Li, W. Color-multiplexing europium doped carbon dots for highly selective and dosage-sensitive cascade visualization of tetracycline and Al^{3+}. *Sens. Actuators, B* **2022**, *362*, 131780.

(16) Fan, Y. J.; Wang, Z. G.; Su, M.; Liu, X. T.; Shen, S. G.; Dong, J. X. A dual-signal fluorescent colorimetric tetracyclines sensor based on multicolor carbon dots as probes and smartphone-assisted visual assay. *Anal. Chim. Acta* **2023**, *1247*, 340843.

(17) Banski, M.; Podhorodecki, A.; Misiewicz, J.; Afzaal, M.; Abdelhady, A. L.; O'Brien, P. Selective excitation of Eu^{3+} in the core of small β-$NaGdF_4$ nanocrystals. *J. Mater. Chem. C* **2013**, *1*, 801−807.

(18) Huang, J.; Wang, X.; Shao, A.; Du, G.; Chen, N. Growth of β-$NaYF_4$:Eu^{3+}crystals by the solvothermal method with the aid of oleic acid and their photoluminescence properties. *Materials* **2019**, *12*, 3711.

(19) Tang, X.; Wang, L.; Ye, H.; Zhao, H.; Zhao, L. Biological matrix-derived carbon quantum dots: Highly selective detection of tetracyclines. *J. Photochem. Photobiol., A* **2022**, *424*, 113653.

(20) Atabaev, T. Sh.; Sayatova, S.; Molkenova, A.; Taniguchi, I. Nitrogen-doped carbon nanoparticles for potential temperature sensing applications. *Sens. Bio-Sens. Res.* **2019**, *22*, 100253.

(21) Molkenova, A.; Kairova, M.; Zhussupbekova, A.; Zhussupbekov, K.; Duisenbayeva, B.; Shvets, I. V.; Atabaev, T. S. Carbon dots doped with barium as a novel contrast agent for efficient CT X-ray attenuation. *Nano-Struct. Nano-Objects* **2022**, *29*, 100839.

(22) Molkenova, A.; Amangeldinova, Y.; Aben, D.; Sayatova, S.; Atabaev, T. S. Quick synthesis of fluorescent nitrogen-doped carbon nanoparticles for selective and sensitive Fe (III) detection in water. *Sens. Bio-Sens. Res.* **2019**, *23*, 100271.

(23) Coates, J. Interpretation of Infrared Spectra, A Practical Approach. In *Encyclopedia of analytical chemistry: Applications, theory, and instrumentation*, 1st ed.; Meyers, R. A., Ed.; John Wiley & Sons: Chichester, 2006; pp 10815−10837.

(24) Mercier, F.; Alliot, C.; Bion, L.; Thromat, N.; Toulhoat, P. XPS study of Eu(III) coordination compounds: Core levels binding energies in solid mixed-oxo-compounds $Eu_mX_xO_y$. *J. Electron Spectrosc. Relat. Phenom.* **2006**, *150*, 21−26.

(25) Yao, R.; Li, Z.; Huo, P.; Gong, C.; Li, J.; Fan, C.; Pu, S. A Eu^{3+}-based high sensitivity ratiometric fluorescence sensor for determination of tetracycline combining bi-functional carbon dots by surface functionalization and heteroatom doping. *Dyes Pigm.* **2022**, *201*, 110190.

(26) Nie, Q.; Deng, J.; Zhou, T. A facile rapid-response and on-site sensor for tetracycline detection in environmental water based on europium-doped carbonized polymer dots. *J. Environ. Chem. Eng.* **2023**, *11*, 109900.

(27) Goponenko, D.; Zhumanova, K.; Shamarova, S.; Yelzhanova, Z.; Ng, A.; Atabaev, T. S. Hydrophobic and luminescent polydimethylsiloxane PDMS-Y_2O_3:Eu^{3+} coating for power enhancement and UV protection of Si solar cells. *Nanomaterials* **2024**, *14*, 674.

(28) Zhumanova, K.; Serik, L.; Molkenova, A.; Atabaev, T. S. UV light blocking and conversion by porous europium-doped titanium dioxide (TiO_2-Eu) thin films for potential protection of photovoltaic devices. *Mater. Today Chem.* **2022**, *26*, 101171.

(29) Tran, N. H.; Chen, H.; Reinhard, M.; Mao, F.; Gin, K. Y.-H. Occurrence and removal of multiple classes of antibiotics and antimicrobial agents in biological wastewater treatment processes. *Water Res.* **2016**, *104*, 461−472.

(30) Pena, A.; Paulo, M.; Silva, L. J. G.; Seifrtová, M.; Lino, C. M.; Solich, P. Tetracycline antibiotics in hospital and municipal wastewaters: a pilot study in Portugal. *Anal. Bioanal. Chem.* **2010**, *396*, 2929−2936.

(31) Li, W.; Zhu, J.; Xie, G.; Ren, Y.; Zheng, Y.-Q. Ratiometric system based on graphene quantum dots and Eu^{3+} for selective detection of tetracyclines. *Anal. Chim. Acta* **2018**, *1022*, 131−137.

https://doi.org/10.1021/acsomega.4c07414
ACS Omega 2025, 10, 619−626

(32) Ti, M.; Li, Y.; Li, Z.; Zhao, D.; Wu, L.; Yuan, L.; He, Y. A ratiometric nanoprobe based on carboxylated graphitic carbon nitride nanosheets and Eu^{3+} for the detection of tetracyclines. *Analyst* **2021**, *146*, 1065−1073.
(33) Maillard, J.; Klehs, K.; Rumble, C.; Vauthey, E.; Heilemann, M.; Fürstenberg, A. Universal quenching of common fluorescent probes by water and alcohols. *Chem. Sci.* **2021**, *12*, 1352−1362.
(34) Ghorai, N.; Bhunia, S.; Burai, S.; Ghosh, H. N.; Purkayastha, P.; Mondal, S. Ultrafast insights into full-colour light-emitting C-Dots. *Nanoscale* **2022**, *14*, 15812−15820.
(35) Ullal, N.; Mehta, R.; Sunil, D. Separation and purification of fluorescent carbon dots − an unmet challenge. *Analyst* **2024**, *149*, 1680−1700.

https://doi.org/10.1021/acsomega.4c07414
ACS Omega 2025, 10, 619−626